

STAR FORMATION IN DISTANT RED GALAXIES: SPITZER OBSERVATIONS IN THE HUBBLE DEEP FIELD SOUTH

TRACY M.A. WEBB¹, PIETER VAN DOKKUM^{2,3}, EIICHI EGAMI⁴, GIOVANNI FAZIO⁵, MARIJN FRANX¹, ERIC GAWISER^{2,3,6}, DAVID HERRERA^{2,3}, JIASHENG HUANG⁵, IVO LABBÉ⁸, PAULINA LIRA⁶, DANILO MARCHESINI^{2,3}, JOSÉ MAZA⁶, RYAN QUADRI², GREGORY RUDNICK⁹, AND PAUL VAN DER WERF¹

Draft version September 6, 2018

ABSTRACT

We present Spitzer 24 μ m imaging of $1.5 < z < 2.5$ Distant Red Galaxies (DRGs) in the $10' \times 10'$ Extended Hubble Deep Field South of the Multiwavelength Survey by Yale-Chile. We detect 65% of the DRGs with $K_{AB} < 23.2$ mag at $S_{24\mu m} \gtrsim 40 \mu Jy$, and conclude that the bulk of the DRG population are dusty active galaxies. A mid-infrared (MIR) color analysis with IRAC data suggests that the MIR fluxes are not dominated by buried AGN, and we interpret the high detection rate as evidence for a high average star formation rate of $\langle SFR \rangle = 130 \pm 30 M_{\odot} yr^{-1}$. From this, we infer that DRGs are important contributors to the cosmic star formation rate density at $z \sim 2$, at a level of $\sim 0.02 M_{\odot} yr^{-1} Mpc^{-3}$ to our completeness limit of $K_{AB} = 22.9$ mag.

Subject headings: galaxies: evolution — galaxies: high-redshift — galaxies: starburst — infrared: galaxies — (ISM:) dust, extinction

1. INTRODUCTION

Through a variety of observational methods we are building a census of the high-redshift universe, and can now directly study galaxies in the process of forming. Color selection criteria effectively select large samples of galaxies at $z > 1$ such as Lyman-break galaxies (LBGs) (Steidel et al. 1996), and the massive Distant Red Galaxies (DRGs) (Franx et al. 2003). Selected by rest-frame optical colors to lie at $z \gtrsim 2$, DRGs exhibit properties of both passively evolved stellar populations and dusty starburst galaxies (Förster Schreiber et al. 2004; Labbé et al. 2005; Papovich et al. 2005). Characterizing this complex population and placing it into the context of the star formation history of the universe will elucidate our overall understanding of the assembly of massive galaxies.

Recent advances in the capabilities of infrared facilities have opened a new window onto the high-redshift universe. Through the direct detection of dust enshrouded activity, mid- and far-infrared (M/FIR) studies provide orthogonal information to that gathered in the ultraviolet (UV), optical and near-infrared (NIR), which can be heavily biased by dust extinction. The work presented here addresses the nature of $z \sim 2$ DRGs through *Spitzer* MIPS-24 μ m and IRAC imaging. We assume a $\Omega_M = 0.3$, $\Omega_{\Lambda} = 0.7$ cosmology and $H_0 = 70 \text{ km s}^{-1} \text{ Mpc}^{-1}$ throughout.

2. THE SAMPLE, SPITZER OBSERVATIONS, AND PHOTOMETRY

The DRG sample was drawn from the $10' \times 10'$ Extended Hubble Deep Field South (EHDF-S) of the Multiwavelength Survey by Yale-Chile (MUSYC) (Gawiser et al. 2005). DRGs are defined by $(J - K)_{\text{vega}} > 2.3$ mag (Franx et al. 2003;

van Dokkum et al. 2003), and, in this paper, we focus on DRGs with $K_{AB} < 23.2$ mag (total magnitudes are given throughout), corresponding to the MUSYC 50% completeness limit (Quadri et al., in preparation).

Photometric redshifts were derived from *UBVRiz'JHK* photometry using the code presented in Rudnick et al. (2001, 2003), through linear combinations of galaxy templates, with an accuracy of $\langle |z_{\text{spec}} - z_{\text{phot}}| / (1 + z_{\text{spec}}) \rangle = 0.05$ for $z > 1.5$. Here, we have restricted our analysis to redshifts $1.5 < z < 2.5$ where the 6.2 μ m, 7.7 μ m, and 8.6 μ m Polycyclic Aromatic Hydrocarbon (PAH) features of star-forming galaxies fall into the Spitzer 24 μ m filter. This provides a sample of 79 DRGs with a median redshift of $z = 2.0$.

The 24 μ m observations were taken in the MIPS photometry mode and consist of 6 separate pointings. The central deepest pointing represents ~ 1 hour of frame time, and the 5 flanking pointings have 35 minutes of frame time each. The raw data were reduced and combined with the Data Analysis Tool developed by the MIPS instrument team (Gordon et al. 2004). The final image covers $\sim 104 \text{ arcmin}^2$.

Imaging at 3.0 μ m, 4.5 μ m, 5.8 μ m and 8.0 μ m was taken in the IRAC mapping mode and mosaicked to produce a $\sim 140 \text{ arcmin}^2$ image. Individual frames of 200 seconds were combined for a final total frame time, per location on the map, of 20 minutes. The Spitzer Science Center provides a Basic Calibrated Data product with flat-field corrections, dark subtraction, and linearity and flux calibrations. Additional steps conducted with the IRAC team customized software included pointing refinement, distortion correction, and mosaicking (Huang et al. 2004).

Photometry on the 24 μ m image was performed using the point spread function (PSF) fitting program DAOPHOT (Stetson 1987). The PSF was characterized using bright isolated point sources and then used to iteratively fit and subtract each object in the image. A small fraction (10/79) DRGs were highly confused with neighboring objects and these were removed from further analysis. We reached an average rms depth of $\sim 13 \mu Jy$, and found the source counts to be in good agreement with Papovich et al. (2004). Because not all the DRGs are detected at 24 μ m, their flux densities and upper limits were determined in a consistent manner by performing aperture photometry at each K -determined position after first

Electronic address: webb@strw.leidenuniv.nl

¹ Leiden Observatory, PO Box 9513, 2300 RA Leiden, The Netherlands

² Department of Astronomy, Yale University, P.O. Box 208101, New Haven, CT 06520-8101

³ Yale Center for Astronomy & Astrophysics, Yale University, P.O. Box 208121, New Haven, CT 06520

⁴ The University of Arizona, Steward Observatory, 933 N. Cherry Ave., Tucson, AZ 85721

⁵ CfA, 60 Garden Street, Cambridge, MA 02138

⁶ Departamento de Astronomía, Universidad de Chile, Casilla, 36-D, Santiago, Chile

⁸ OCIW, 813 Santa Barbara Street, Pasadena, CA, 91101

⁹ NOAO, 950 N. Cherry Ave., Tucson, AZ, 85719

subtracting all other objects in the catalog. We used $6''$ diameter apertures, and used the PSF stars to apply an aperture correction factor to total flux densities at $40''$.

Due to the smaller beam size at the shorter IRAC wavelengths ($< 2''$), and because highly confused DRGs have been removed from the sample, PSF fitting was not employed for the IRAC measurements. Aperture photometry ($3''$ diameter) was performed at the location of each DRG for each IRAC channel, again using isolated point sources to determine aperture corrections to total fluxes at $12.2''$. The average rms depths are $2.6\mu\text{Jy}$, $2.7\mu\text{Jy}$, $4.3\mu\text{Jy}$ and $4.0\mu\text{Jy}$ at $3.6\mu\text{m}$, $4.5\mu\text{m}$, $5.8\mu\text{m}$, and $8.0\mu\text{m}$, respectively.

3. MIR CONSTRAINTS ON THE NATURE OF DRGS

At $1.5 < z < 2.5$, the $24\mu\text{m}$ filter samples $\sim 6\text{--}10\mu\text{m}$ in the rest-frame and the $24\mu\text{m}$ flux offers a powerful method of differentiating between two basic SED types: active dusty galaxies, i.e., those that are powered by either star formation or active galactic nuclei (AGN), both of which produce substantial mid-infrared emission, and passively evolved systems whose stellar flux drops drastically longward of $\sim 2\mu\text{m}$ (see Fig. 1). In pure starburst galaxies, the MIR emission is dominated by PAH features which are strong relative to the underlying dust continuum, which only begins to rise above $\sim 10\mu\text{m}$. The hard radiation field of an AGN destroys PAH carriers and the continuum emission from hot small dust grains is strong throughout the MIR (Genzel & Cersarsky 2000).

In Fig. 1 we show the $24\mu\text{m}$ flux densities for the DRGs, normalized to their rest-frame L_V , and overlaid with three template SEDs; 65% are detected at $24\mu\text{m}$ and the remainder are shown as 3σ upper limits. This detection rate is in line with that found by (Papovich et al. 2005) for DRGs the GOODS Chandra Deep Field South, to a similar depth. All of the $24\mu\text{m}$ -detected DRGs are incompatible with old stellar populations and dusty starburst or AGN galaxies are required to produce such strong mid-IR emission. The sample shows a wide range in $24\mu\text{m}$ flux which we interpret primarily as a range in star formation rates. However, a real difference in PAH strengths, relative to the continuum, due to a range in metallicity or the hardness of the radiation field (e.g., Engelbracht et al. 2005; Hogg et al. 2005) could also be important, as could a variation in the level of AGN contamination of the MIR flux, though as we discuss below we deem this latter possibility unlikely.

The SEDs of DRGs which are not detected at $24\mu\text{m}$ (35%) are consistent with passively evolved systems, but also lower luminosity or less dusty starbursts, or starbursts which have weak or absent PAH signatures as explained above. To investigate the nature of the $24\mu\text{m}$ -faint DRGs we used a stacking analysis to measure their mean $24\mu\text{m}$ emission and find $S_{24\mu\text{m}} = 10 \pm 2 \mu\text{Jy}$. Thus, the remaining 35% of the sample cannot be entirely composed of passively evolved systems but contains some fraction of dusty starburst or AGN galaxies. A bootstrapping analysis indicates that this measurement is not dominated by a small number of systems, but beyond this we cannot constrain the fraction of starburst or AGN systems within this group.

Combining the $24\mu\text{m}$ measurements with IRAC data provides a color diagnostic of AGN activity (Fig. 2) (Ivison et al. 2004; Egami et al. 2004; Huang et al. 2005). This technique relies on the different rest-frame NIR SED properties of AGN and starburst galaxies: stellar emission in starburst galaxies leads to a relatively flat SED in the rest-frame NIR, while hot dust around an AGN produces a power-

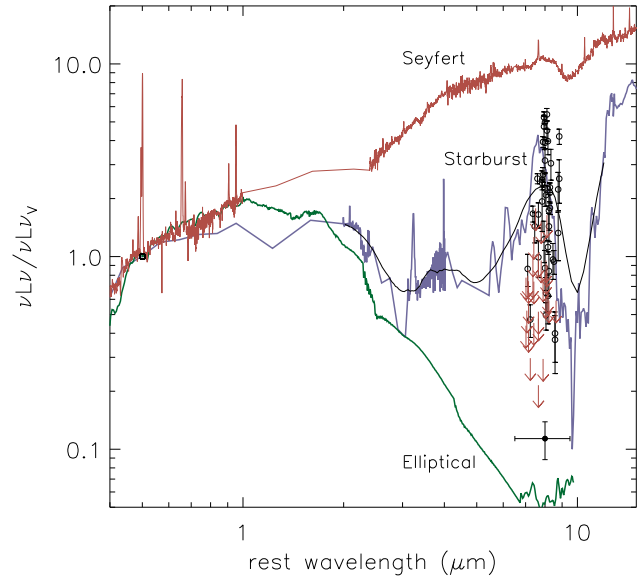


FIG. 1.— The $24\mu\text{m}$ fluxes or limits of the DRGs, normalized to their rest-frame L_V . Points are DRGs with $24\mu\text{m}$ detections, and arrows show 3σ upper-limits for the remainder. The single solid point below the arrows denotes the stacked measurement of DRGs which are not individually detected. Three SEDs are shown: the green line corresponds to an elliptical galaxy model (Coleman, Wu, & Weedman 1980) extrapolated to longer wavelengths using ISO observations of local ellipticals; the blue line to the observed SED of Arp220; and the red line to the observed SED of NGC1068 (Jiasheng Huang, personal communication). Because of the rapid variation in flux with wavelength for the Arp 220 SED in the MIR we also show this SED smoothed by the $24\mu\text{m}$ filter transmission curve (smooth black line).

law that increases toward longer wavelengths. We have detected 50% of the $24\mu\text{m}$ -bright DRGs at $4.5\mu\text{m}$ and $8\mu\text{m}$, another 20% at $4.5\mu\text{m}$, but not $8.0\mu\text{m}$, 5% in neither, and 25% fall off the IRAC channel 2/4 field-of-view. The colors (Fig. 2) indicate that star formation dominates the MIR emission of the DRGs, but as a conservative cut we consider the four objects with $S_{8\mu\text{m}}/S_{4.5\mu\text{m}} > 1.5$ to have possible AGN contamination. This is in agreement with results from the X-ray (Rubin et al. 2004; Reddy et al. 2005) and optical (van Dokkum et al. 2003) which also indicate that AGN do not significantly contribute to the observed luminosity of DRGs. It should be remembered, however, that very heavily obscured or weak AGN, though energetically unimportant in terms of observed MIR properties, may still be present.

4. STAR FORMATION RATES OF DRGS

PAH and MIR emission can be used to estimate the current star formation rate (SFR) of a galaxy (Wu et al. 2005). Using an Arp220 SED template we extrapolated from $24\mu\text{m}/(1+z)$ to rest-frame $6.75\mu\text{m}$. We then estimated L_{IR} through the $6.75\mu\text{m}$ - F_{FIR} relation calibrated locally with the *Infrared Space Observatory*, which shows a scatter of $\sim 50\%$ (Elbaz et al. 2002). This value can then be converted to a SFR following the L_{IR} -SFR relationship of Kennicutt (1998) with an uncertainty of a factor $\sim 2\text{--}3$. We note that adopting an M82-like SED instead of Arp220 in the first step results in SFR estimates which are systematically $1.4\times$ lower.

In Fig. 3 we plot the $24\mu\text{m}$ star formation rates or upper limits of the individual DRGs with redshift. The population is not homogeneous and individual galaxies range in SFR from $< 30 M_{\odot}\text{yr}^{-1}$ to $\sim 1000 M_{\odot}\text{yr}^{-1}$. A strong AGN contribution to the MIR flux will contaminate this estimate, by boosting

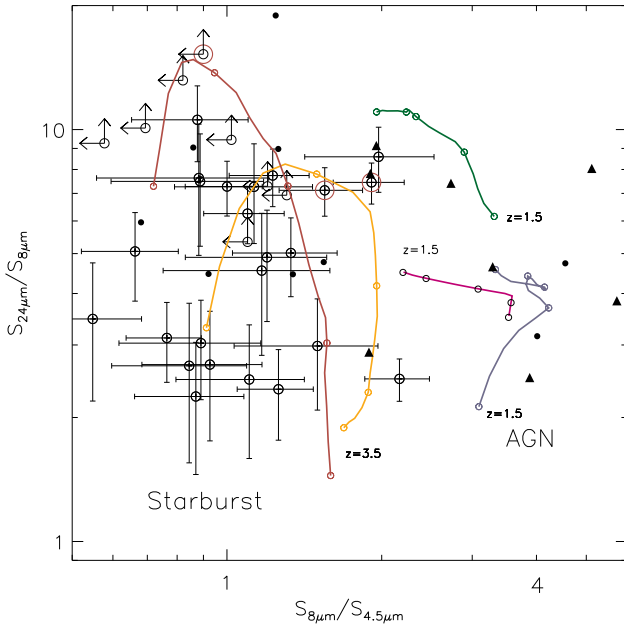


FIG. 2.— A MIR color-color plot. The tracks correspond to two starburst SEDs (left-most, orange-Arp220; red-M82) and three AGN dominated SEDs (right-most, magenta-MRK231; purple-Seyfert 1 NGC5506; green-Seyfert 2 NGC1068). The SED tracks begin at $z = 1.5$ and are marked by circles in $z = 0.5$ steps, to $z = 3.5$. The open points show DRGs from this work which are detected at $24\mu\text{m}$, with the radio detected objects indicated by the large red circles. Also shown are Spitzer observed SMGs (solid circles; Egami et al. 2004) and optically-faint AGN (solid triangles; Rigby et al. 2005).

the inferred SFR, and sources which may contain AGN are marked. Also highlighted are three DRGs which are detected in the deep radio map of Huynh et al. (2005), two of which are possible AGN based on their MIR colors. Studies indicate that the fraction of AGN contamination in the μJy radio population increases at higher redshift (Richards 2000; Garrett 2001), and thus, the radio detected DRGs may indeed contain weak AGN. However, we note that these systems fall within 1σ of the FIR/radio flux correlation of Condon (1992) (with no systematic offset), which only holds for starburst galaxies, and thus significant AGN contamination is unlikely.

Using a stacking analysis, we calculated an average SFR for the entire DRG sample of $\langle \text{SFR} \rangle = 130 \pm 30 M_{\odot} \text{yr}^{-1}$. This is the uncertainty-weighted mean of *all* 69 DRGs, assuming no AGN contamination and a mean redshift of $z = 2$, with the uncertainty in the mean estimated from a bootstrapping analysis. This result is in good agreement with the optical SED modeling results of Förster Schreiber et al. (2004) of $120 M_{\odot} \text{yr}^{-1}$, and X-ray and submillimeter stacking analyses which estimate $\sim 100\text{--}200 M_{\odot} \text{yr}^{-1}$ and $\sim 100 M_{\odot} \text{yr}^{-1}$, respectively (Rubin et al. 2004; Reddy et al. 2005; Knudsen et al. 2005).

A significant source of error in this calculation is the photometric redshift uncertainty, since the rest-frame flux of starburst galaxies changes rapidly with wavelength in the region surrounding the PAH features. This effect was quantified by recalculating SFRs for simulated redshifts within Gaussian confidence intervals, and the resulting uncertainties are shown in Fig. 3. The uncertainties are substantial, ranging from a factor of two to almost an order of magnitude.

We calculated the optically normalized star formation rates (SFR/L_V) for the DRGs, which provide an indication of their

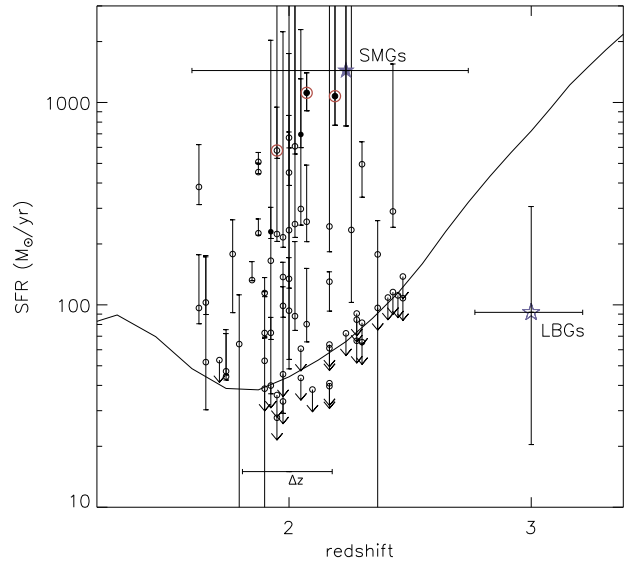


FIG. 3.— The SFRs for DRGs as a function of redshift (circles). Filled circles mark DRGs which may contain AGN, and red circles mark radio detected galaxies. The solid line corresponds to the average effective SFR depth as a function of redshift, for these data. Also shown for reference is the median SFR for radio-detected submm galaxies from Chapman et al. (2005) (solid star) and that of Lyman-break galaxies from Shapley et al. (2001) (open star).

age and/or dust content. We find $\langle \text{SFR}/L_V \rangle \sim 19^9$, which is in excellent agreement with the submillimeter study of DRGs by Knudsen et al. (2005), who measure $\langle \text{SFR}/L_V \rangle \sim 20$. However, the values for the DRGs show large scatter, ranging from $\text{SFR}/L_V < 5$ to 200. Monte Carlo simulations indicate that the redshift uncertainties cannot account for the full range of this scatter and, moreover, the three radio detected galaxies have the highest SFR/L_V , for a given L_V ; as their radio flux confirms that they are extreme systems, their high SFR/L_V values are unlikely to stem solely from redshift uncertainties.

5. CONTRIBUTION TO THE COSMIC STAR FORMATION DENSITY

Using the $24\mu\text{m}$ SFR estimates presented here, and the number density of DRGs in the MUSYC fields (known to a factor of two; Quadri et al., in preparation), we estimate a star formation rate density (SFRD) for the DRGs of $\sim 0.02 M_{\odot} \text{yr}^{-1} \text{Mpc}^{-1}$ over the redshift range $1.5 < z < 2.5$, and to a depth of $K_{AB} = 22.9$ mag. At this depth our sample is 100% complete, and therefore requires no completeness correction. A number of uncertainties affect this estimate, including those described in the previous sections: errors in the photometric redshifts, the uncertain conversion of an observed $24\mu\text{m}$ flux to a SFR, and the potential contamination from AGN. Also important are possible differences in dust properties and the Initial Mass Function from low to high redshift, which are difficult to quantify. Nevertheless, though the uncertainties in the individual star formation rates are high, the average star formation rate of the population is known to better accuracy since the redshift uncertainties, at least, are largely statistical.

The total SFRD, integrated over all galaxies, provides a census of the star formation history of the universe, and the relative contributions of different galaxy populations is indicative of their importance in assembling stellar mass. In a general sense, there is now reasonable agreement be-

⁹ $M_{\odot} \text{yr}^{-1} (L_{\odot} \times 10^{-10})^{-1}$

tween IR and optical SFRD estimates at $z \sim 2$. Reddy et al. (2005) estimate a SFRD (from X-ray measurements) of $0.10 \text{ M}_{\odot} \text{ yr}^{-1} \text{ Mpc}^{-3}$ over $1.4 < z < 2.6$, for optical and NIR selected galaxies, with DRGs producing 20% of this total. Likewise, Chapman et al. (2005) estimate $\sim 0.1 \text{ M}_{\odot} \text{ yr}^{-1} \text{ Mpc}^{-3}$ for submm-selected systems, after extending the submm luminosity function down to $S_{850\mu\text{m}} = 1 \text{ mJy}$, and applying a correction for AGN contamination. Thus, the two techniques converge on a similar value, and assuming the $S_{850\mu\text{m}} \sim 1 \text{ mJy}$ population encompasses the bulk of the optical and NIR selected galaxies, and vice versa, this can be taken as a total SFRD at $z \sim 2$ (but see both papers for a discussion of uncertainties and assumptions).

Our completeness limit of $K_{\text{AB}} = 22.9 \text{ mag}$ is roughly equal to the Reddy et al. (2005) DRG depth over a similar redshift range, and we find the same SFRD for DRGs of $\sim 0.02 \text{ M}_{\odot} \text{ yr}^{-1} \text{ Mpc}^{-3}$; thus, the X-ray and MIR determined SFRD measurements agree that the DRGs produce roughly 20% of the total SFRD of optical and NIR selected star forming galaxies. A consistent picture is seen at longer wavelengths. If we use the $24\mu\text{m}$ flux density of each DRG to predict its approximate $850\mu\text{m}$ flux density, we find that our SFRD estimate is dominated by objects with $S_{850\mu\text{m}} > 1 \text{ mJy}$, and thus again DRGs produce $\sim 20\%$ of the total SFRD as measured at submm wavelengths. In conclusion, DRGs, to a depth of $K_{\text{AB}} = 22.9 \text{ mag}$ are important contributors to the total SFRD at $z \sim 2$, and by extension, to the assembly of massive galaxies.

6. SUMMARY

The analysis presented here indicate that DRGs constitute a heterogeneous population, with the majority consisting of luminous and dusty starburst galaxies. We find that $>65\%$ of the E-HDFS sample are such systems and this is in good agreement with similar Spitzer studies (Papovich et al. 2005), and rest-frame optical SED modeling (Förster Schreiber et al. 2004; Labbé et al. 2005). Using the $24\mu\text{m}$ flux we estimate an average SFR for the population (to $K_{\text{AB}} = 23.2$) of $130 \pm 30 \text{ M}_{\odot} \text{ yr}^{-1}$, in line with earlier estimates from optical, submm and X-ray studies. Normalizing the SFR to the rest-frame L_V yields $\text{SFR}/L_V \sim 19 \text{ M}_{\odot} \text{ yr}^{-1} (L_{\odot} \times 10^{-10})^{-1}$, but with substantial scatter around this value. The scatter cannot be explained solely by redshift uncertainties, and indicates a real difference in the individual properties DRGs. Overall, DRGs are important contributors to the SFRD at $z \sim 2$ at a level of $0.02 \text{ M}_{\odot} \text{ yr}^{-1} \text{ Mpc}^{-3}$ to our 100% completeness limit of $K_{\text{AB}} = 22.9$.

Research by TW is supported by a VENI Research Fellowship, through the Nederlandse Organisatie voor Wetenschappelijk Onderzoek. DM is supported by NASA LTSA NNG04GE12G. We are grateful to N.M. Förster Schreiber for a careful reading and insightful comments on an early version of this work.

REFERENCES

- Chapman, S. C, Blain, A. W., Smail, I., & Ivison, R. J. 2005, *ApJ*, 622, 772
 Coleman, G. D., Wu, C. -C., & Weedman, D. W. 1980, *ApJS*, 43, 393
 Condon, J.J., 1992, *ARA&A*, 30, 575
 Egami, E., et al. 2004, *ApJS*, 154, 130
 Elbaz, D., Cesarsky, C. J., Chantal, P., Aussel, H., Franceschini, A., Fadda, D., & Chary, R. R. 2002, *A&A*, 384, 848
 Engelbracht, C. W., Gordon, K. D., Rieke, G. H., Werner, M. W., Dale, D. A., & Latter, W. B. 2005, *ApJ*, 628, L29
 Förster Schreiber, N. M. et al., 2004, *ApJ*, 616, 40
 Franx, M. et al., 2003, *ApJ*, 587, 79L
 Garret, M. A. 2001, in *ASP Conf Ser.* 249, *The Central kpc of Starbursts and AGN*, ed. J. H. Knapen, J. E. Beckman, I. Shlosman, & T. J. Mahoney, 652
 Gawiser, E. et al. 2005, submitted to *ApJ*, astro-ph/0509202
 Genzel, R. & Cesarsky, C. J. 2000, *ARA&A*, 38, 761
 Gordon, K. D. et al. 2005, *PASP*, 117, 503
 Hogg, D. W., Tremonti, C. A., Blanton, M. R., Finkbeiner, D. P., Padmanabhan, N., Quintero, A. D., Schlegel, D. J., & Wherry, N. 2005, *ApJ*, 624, 162
 Huang, J. -S. et al. 2004, *ApJS*, 154, 44
 Huang, J. et al., 2005, *ApJ*, in press
 Huynh, M., Jackson, C. A., Norris, R., & Prandoni, I. 2005, *AJ*, 130, 1373
 Ivison, R. J. et al. 2004, *ApJS*, 154, 124
 Kennicutt, R. C., Jr. 1998, *ApJ*, 498, 541
 Knudsen, K. K. et al. 2005, submitted to *ApJ*
 Labbé, I. et al. 2005, *ApJ*, 624, 81L
 Papovich, C. et al. 2004, *ApJS*, 154, 70
 Papovich, C. et al. 2005, *ApJ*, in press
 Reddy, N. A., Erb, D. K., Steidel, C. C., Shapley, A. E., Adelberger, K. L., & Pettini, M. 2005, *ApJ*, 633, 748
 Richards, E. A. 2000, *ApJ*, 533, 611
 Rigby, J. R. et al. 2005, *ApJ*, 627, 134
 Rudnick, G. et al. 2001, *AJ*, 122, 2205
 Rudnick, G. et al. 2003, *ApJ*, 599, 847
 Rubin, K. H.R., van Dokkum, P. G., Coppi, P., Johnson, O., Förster Schreiber, N. L., Franx, M., & van der Werf, P. 2004, *ApJ*, 613, 5
 Shapley, A. E. et al. 2001, *ApJ* 562, 95
 Steidel, C. C., Adelberger, K. L., Giavalisco, M., Dickinson, M., & Pettini, M. 1996, *ApJ*, 519, 1
 Stetson, Peter, B. 1987, *PASP*, 99, 191
 van Dokkum, P. G. et al. 2003, *ApJ*, 587, 83L
 Wu H. et al. 2005, *ApJ*, 632, 79